Nanoscale Res Lett (2008) 3:201–204
DOI 10.1007/s11671-008-9136-2

NANO PERSPECTIVES

Converting Layered Zinc Acetate Nanobelts to One-dimensional Structured ZnO Nanoparticle Aggregates and their Photocatalytic Activity

Ye Zhang · Feng Zhu · Junxi Zhang · Lingli Xia

Received: 4 May 2008 / Accepted: 30 May 2008 / Published online: 18 June 2008
© to the authors 2008

Abstract We were successful in synthesizing periodic layered zinc acetate nanobelts through a hydrothermal solution process. One-dimensional structured ZnO nanoparticle aggregate was obtained by simple thermal annealing of the above-mentioned layered ZnO acetate nanobelts at 300 °C. The morphology, microstructure, and composition of the synthesized ZnO and its precursors were characterized by transmission electron microscopy (TEM), X-ray diffraction (XRD), and infrared spectroscopy, respectively. Low angle X-ray diffraction spectra reveal that as-synthesized zinc acetate has a layered structure with two interlayer d-spacings (one is 1.32 nm and the other is 1.91 nm). SEM and TEM indicate that nanobelt precursors were 100–200 nm in width and possesses length up to 30 μm. Calcination of precursor in air results in the formation of one-dimensional structured ZnO nanoparticle aggregates. In addition, the as-prepared ZnO nanoparticle aggregates exhibit high photocatalytic activity for the photocatalytic degradation of methyl orange (MO).

Keywords Nanostructures · Hydrothermal crystal growth · Nanomaterials · Semiconducting II–VI materials

Y. Zhang (✉) · F. Zhu · J. Zhang
Key Laboratory of Materials Physics, and Anhui Key Laboratory of Nanomaterials and Nanostructures, Institute of Solid State Physics, Chinese Academy of Sciences, Hefei 230031, People's Republic of China
e-mail: yezhang@issp.ac.cn

L. Xia
Basic Experiment Center, Fundamental Department, Artillery Academy P.L.A, Hefei, People's Republic of China

Introduction

ZnO is one of the most important wide band gap (3.37 at room temperature) semiconductors because of its promising potential applications in room temperature UV lasers [1], sensors [2, 3], solar cells [4, 5], transparent electrodes [6], and piezoelectric actuators [7]. In recent years, regulating the shape of semiconductor nanostructures has been a subject of intensive research because it provides an effective strategy for tuning the electronic, magnetic, optical, and catalytic properties of a semiconductor. For example, Duan et al. successfully synthesized zigzig SnO_2 nanobelts via physical vapor deposition method [8]. Pan et al. prepared single-crystal CdS_xSe_{1-x} nanobelts and investigated their optical properties [9]. Orthorhombic $Pb_3O_2Cl_2$ (mendipite) nanobelts were synthesized via a solventless thermolysis of a single-source precursor in the presence of capping ligands by Sigman et al. [10]. Venugopal et al. also fabricated single crystalline nanobelts via laser ablation assisted chemical vapor deposition (CVD) method [11]. It is worthy to mention that S. H. Yu' group successfully synthesized single-crystal $CuGeO_3$ nanobelts with a layered mesostructure via a simple hydrothermal route [12]. Chen et al. also synthesized Tungstate-based inorganic–organic hybrid nanobelts/nanotubes with highly ordered lamellar mesostructures and tunable interlayer distances in nonpolar solvents [13]. Layered structure makes it easy to intercalate different elements into the interlayer space [14]. Then, layered structures combined with belt-like morphology would provide opportunities for developing new types of nanostructures that are doped with different elements. In this paper, we show that periodic layered zinc acetate nanobelts can be synthesized by a facile hydrothermal solution method.

In addition, one-dimensional structured ZnO nanoparticle aggregate was obtained by calcination of the precursor in air. ZnO can be used as photocatalytical semiconductor due to a band gap, which can be activated by UV-irradiation [15]. Under UV-irradiation, holes and electrons are yielded which possess an oxidation potential large enough to generate OH• radicals or O_2^-. In this paper, the photocatalytic properties of ZnO nanoparticle aggregates are studied at length.

Experimental Section

All chemicals were analytical grade and used as received without further purification. In a typical synthesis, 4.0 g zinc acetate, 3.6 g CTAB, and 180 g deionized water were added into a 200 mL beaker. Under vigorous magnetic stirring, ammonia (25 wt%) was dropped into the solution to increase pH value to 8.2. White precipitation was yielded. Then, the solution were transferred to a Teflon-lined stainless steel autoclave and sealed tightly. The autoclave was kept in an oven with temperature 50 °C for 24 h. White gel-like precipitation was found deposited on the bottom of the Teflon cup. After filtration, the precipitate was washed (three times) thoroughly with distilled water and ethanol to remove any alkaline salt and surfactants that remained in the final products and dried at room temperature in air for 12 h. Paper-like products formed on the filter paper. Thermal treatments were carried out at 300 °C in air for 1 h. The as-prepared samples were characterized by field emission scanning electron microcopy (SEM) (SEM: Sirion 200 FEG), transmission electron microscopy (TEM) (JEOL 2010, accelerating voltage of 200 kV), selected-area electron diffraction (SAED) (JEOL 2010, accelerating voltage of 200 kV). X-ray diffraction spectra (XRD) (Philips X'pert-PRO, Cu Kα (0.15419 nm) radiation), and infrared spectroscopy. (Cary 5E UV–vis–NIR spectrophotometer).

Aqueous suspensions employed in photocatalytic experiments usually contained 3 g L^{-1} of as-synthesized ZnO nanoparticles and a 10 mg L^{-1} concentration of methyl orange. All kinetic experiments were performed under atmospheric conditions and constant magnetic stirring. The ZnO suspensions with methyl orange were illuminated continuously with light from a 30 W mercury lamp (2,537 Å). The distance between lamp and suspension is ~10 cm.

Results and Discussions

Layered Structured Zinc Acetate Nanobelts

Zinc acetate nanobelts were synthesized via a mild hydrothermal solution process at 50 °C. Nanobelt-like structures were characterized by TEM (Fig. 1). The average width of the nanobelts was 100–200 nm, and their lengths ranged from 10 to 30 μm. Growth temperature plays a key role in formation of nanobelt-like morphology. Temperature higher than 80 °C only resulted in the formation of microwhiskers or sheetlike structures. pH value is also important. pH value higher than 9 or lower than 7 results in no precipitates in solution. Low angle XRD pattern of as-synthesized zinc acetate nanobelts is shown in Fig. 2. The strongest diffraction peak at $2\theta = 6.7°$ corresponds to an interlayer d-spacing of 1.32 nm (the $001^{(a)}$ diffraction of layered structure) and another diffraction peak at $2\theta = 4.4°$ accords with the other interlayer d-spacing of 1.91 nm (the $001^{(b)}$ diffraction of layered structure). The peaks at 8.8°, 13.3°, and 20.1° can be attributed to the second and third order diffraction of (00l) plane of $Zn(OH)_x(CH_3COO)_y \cdot zH_2O$, respectively. Since it is convenient to introduce ions, such as N^{3-}, Mg^{2+}, Cd^{2+}, Mn^{2+}, to the interlayer spacing by ionic exchange reaction, this hierarchically structured zinc acetate as precursor of ZnO looks promising future for fabricating

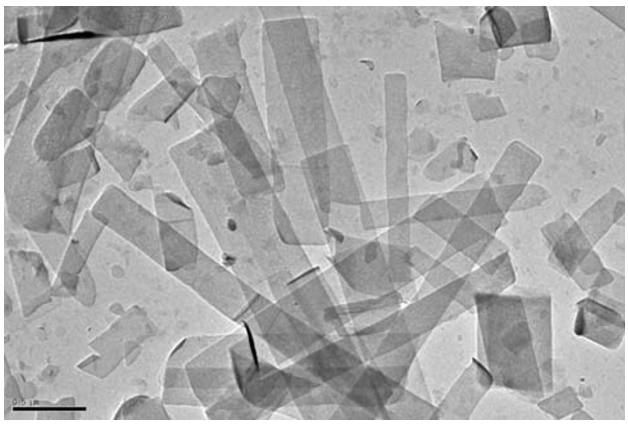

Fig. 1 TEM images of as-synthesized zinc acetate nanobelts at different magnifications. Scale bar: 0.5 μm

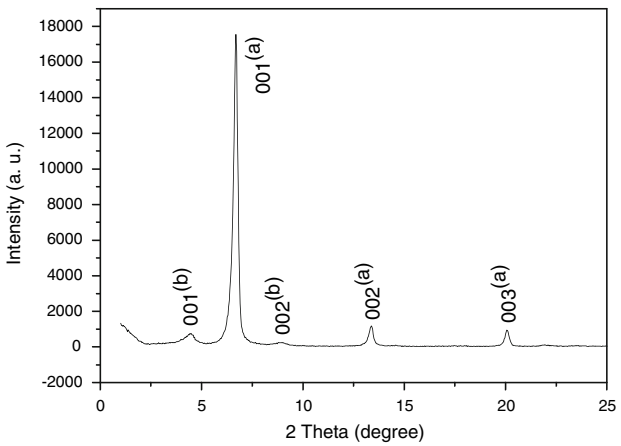

Fig. 2 Low angle XRD pattern of as-synthesized zinc acetate nanobelts

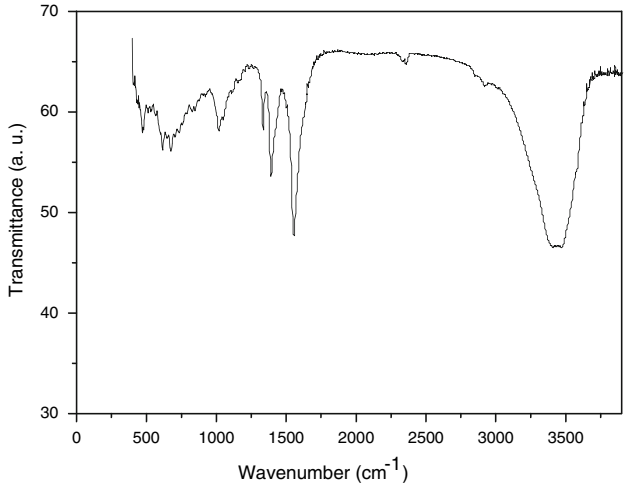

Fig. 3 IR spectrum of as-synthesized zinc acetate nanobelts

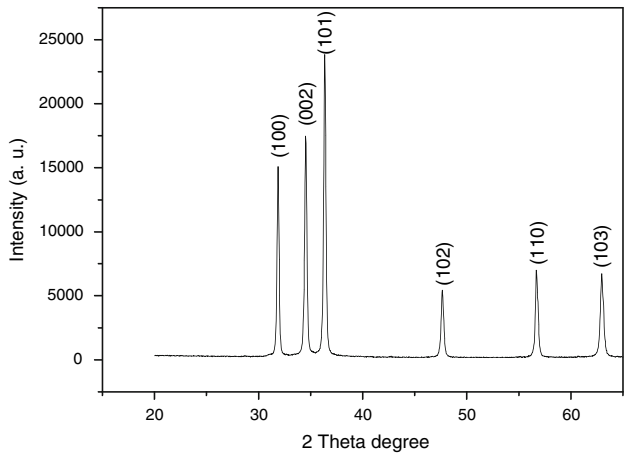

Fig. 4 XRD pattern of ZnO nanoparticle aggregate obtained by thermal treatment at 300 °C in air

functional electrical device. Infrared spectroscopy of zinc acetate (Fig. 3) was also measured to give information of the CH_3COO group and OH group within the interlayer. The broad absorption band at 3,420 cm^{-1} can be assigned to the OH group and water. The two weak peaks at 2,920 and 2,850 cm^{-1} are due to the C–H stretching band. The absorption band at 1,550 cm^{-1} originates from the antisymmetric COO^- stretching vibration. The band at 1,390 cm^{-1} is attributed to the symmetric COO^- stretching vibration mode. The bands at 1,340 and 1,010 cm^{-1} can be assigned to the deformation and rocking modes of the CH_3 group [16–19]. The difference between antisymmetric COO^- stretching vibration band and symmetric COO^- stretching vibration band is 160 cm^{-1}. This large difference means that COO^- is in monodentate state rather than free group state. It is suggested that the coordination of the COO groups to zinc cations for layered zinc acetate is monodentate. In another word, acetate anions are coordinated to polynuclear zinc hydroxyl layers in a monodentate manner.

One-dimensional Structured ZnO Nanoparticles Aggregate

ZnO was obtained by calcinations of the above precursor in air at 300 °C. XRD pattern demonstrates that the produced product shows a high-quality wurtzite ZnO structure, as shown in Fig. 4. Compared with the XRD pattern of precursor, no diffraction peaks appear in the low angle range. It means layer structure collapses under heat treatment. TEM images (Fig. 5) show that chain-like ZnO nanoparticle aggregates were formed under calcinations. The nanoparticle size measured from the TEM image is 10–25 nm. The average crystallite size for ZnO nanoparticle was also determined from the linewidth broadening of the XRD peak corresponding to (002) reflection, using the Debye–Scherrer equation. The value of crystal size is 20 nm, which is consistent with the result of TEM observation.

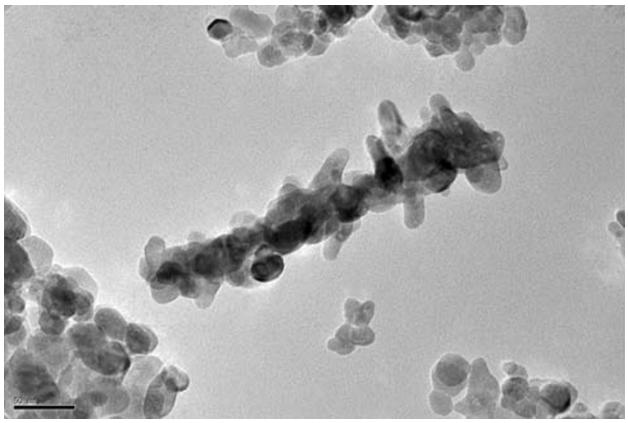

Fig. 5 TEM images of one-dimensional ZnO nanoparticle aggregate. Scale bar: 50 nm

Photocatalytic Degradation of Methyl Orange (MO) by One-dimensional Structured ZnO Nanoparticle Aggregates

Methyl orange ($C_{14}H_{14}N_3 \cdot SO_3Na$) is one of the representative azo class of dyes, which are the most important class of synthetic organic dyes used in the textile industry and are also common industrial pollutants. The photocatalytic properties of ZnO nanoparticle on degradation of methyl orange were studied. Extent of photocatalytic degradation was determined by the reduction in absorbance of the solution. Figure 6 shows a typical time-dependent UV–vis spectrum. The absorption peaks corresponding to the dye diminished after 2 h photoirradiation. The rapid disappearance of the absorption band in Fig. 6 suggests

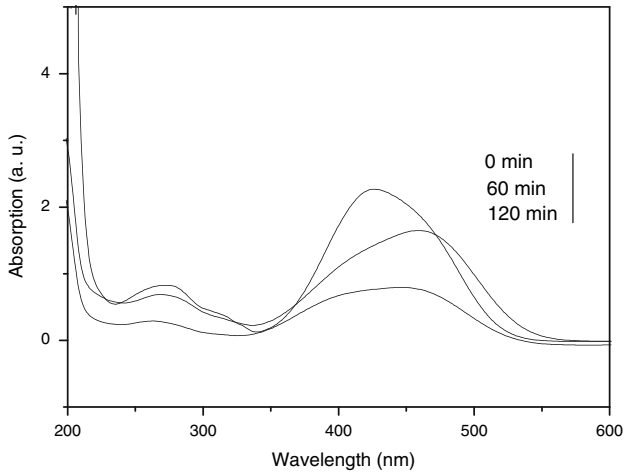

Fig. 6 UV–vis spectrum of ZnO/methyl orange solution

that the functional group responsible for the characteristic color of the MO dye is broken down. Since the power of UV lamp we used is very low (only 30 W), nanoparticle aggregates present high photocatalytic degradation efficiency to methyl orange. The reason is as follows: it is known that the photocatalytic activity of ZnO is strongly dependent on the growth direction of the crystal plane. Polar plane of ZnO exhibits higher photocatalytic activity than nonpolar plane of ZnO [20]. After calcinations, the polar (001) Zn planes of ZnO emerge on the surface of aggregate. An increase of polar Zn (0001) or O (0001) faces leads to a significant enhancement of photocatalytic activity of ZnO.

Conclusion

In summary, hierarchically structured zinc acetate nanobelts were successfully synthesized via a mild hydrothermal method. The zinc acetate nanobelts possess layered structure with two interlayer d-spacings (1.32–1.91 nm). Acetate anions are coordinated to polynuclear zinc hydroxyl layers in a monodentate manner. Nanobelt precursors are 100–200 nm in width, 10–20 nm in thickness, and possess length up to 30 μm. The layered ZnO acetate nanobelts were successfully converted to one-dimensional structured ZnO nanoparticle aggregate through simple thermal treatment of the above-mentioned precursor at 300 °C. The nanoparticle size is 10–25 nm. Photocatalytic experiment indicated that UV/one-dimensional ZnO nanoparticle aggregate process could be efficiently used to degrade azo class of dyes, such as MO.

Acknowledgements Authors acknowledge the support from the National Key Project of Fundamental Research for Nanomaterials and Nanostructures (Grant No. 2005CB623603) and Natural Science Foundation of Anhui (Grant No. 070414196).

References

1. M.H. Huang, S. Mao, H. Feick, H. Yan, Y. Wu, H. Kind et al., Science **292**, 1897 (2001). doi:10.1126/science.1060367
2. J.F. Zang, C.M. Li, X.Q. Cui, J.X. Wang, X.W. Sun, H. Dong et al., Electroanalysis **19**, 1008 (2007). doi:10.1002/elan.200603808
3. R. Ferro, J.A. Rodriguez, P. Bertrand, Physica Status Solidi C **2**, 3754 (2005)
4. D.L. Young, J. Keane, A. Duda, J.A.M. AbuShama, C.L. Perkins, M. Romero, R. Noufi, Prog. Photovolt. Res. Appl. **11**, 535 (2003). doi:10.1002/pip.516
5. C. Calderon, G. Gordillo, J. Olarte, Physica Status Solidi B **242**, 1915 (2005). doi:10.1002/pssb.200461747
6. H. Iechi, T. Okawara, M. Sakai, M. Nakanura, K. Kudo, Electr. Eng. Jpn. **158**, 49–55 (2007)
7. Z.L. Wang, J.H. Song, Science **312**, 242 (2006). doi:10.1126/science.1124005
8. J.H. Duan, S.G. Yang, H.W. Liu, J.F. Gong, H.B. Huang, X. Zhao et al., J. Am. Chem. Soc. **127**, 6180 (2005). doi:10.1021/ja042748d
9. A.L. Pan, H. Yang, R.B. Liu, R. Yu, B.S. Zou, Z.L. Wang, J. Am. Chem. Soc. **127**, 15692 (2005). doi:10.1021/ja056116i
10. M.B. Sigman, B.A. Korgel, J. Am. Chem. Soc. **127**, 10089 (2005). doi:10.1021/ja051956i
11. R. Venugopal, P.I. Lin, C.C. Liu, Y.T. Chen, J. Am. Chem. Soc. **127**, 11262 (2005). doi:10.1021/ja044270j
12. R.Q. Song, A.W. Xu, S.H. Yu, J. Am. Chem. Soc. **129**, 4152 (2007). doi:10.1021/ja070536 l
13. D.L. Chen, Y. Sugahara, Chem. Mater. **19**, 1808 (2007). doi:10.1021/cm062039u
14. Y. Wang, G.Z. Cao, Chem. Mater. **18**, 2787 (2006). doi:10.1021/cm052765 h
15. E.S. Jang, J.H. Won, S.J. Hwang, J.H. Choy, Adv. Mater. **18**, 3309 (2006). doi:10.1002/adma.200601455
16. P. Baraldi, G. Fabbri, Spectrochim. Acta. A Mol. Biomol. Spectrosc. **37**, 89 (1981). doi:10.1016/0584-8539(81)80092-X
17. K. Scott, Y. Zhang, R. Wang, A. Clearfield, Chem. Mater. **7**, 1095 (1995). doi:10.1021/cm00054a008
18. K. Nakamoto, *Infrared and Raman Spectra of Inorganic and Coordination Compounds*, 4th edn. (Wiley, New York, 1986)
19. A.S. Milev, G.S.K. Kannangara, M.A. Wilson, Langmuir **20**, 1888 (2004). doi:10.1021/la0355601
20. E.S. Jang, J.H. Won, S.J. Hwang, J.H. Choy, Adv. Mater. **18**, 3309 (2006). doi:10.1002/adma.200601455